Key Engineering Materials
ISSN: 1662-9795, Vol. 926, pp 906-916
doi:10.4028/p-u6g3p6

Submitted: 2021-12-05
Revised: 2022-01-17
Accepted: 2022-02-04
Online: 2022-07-22

Failure Prediction of Automotive Components Utilizing a Path Independent Forming Limit Criterion

Alexander Barlo[1,a*], Mats Sigvant[1,2,b], Niko Manopulo[3,c], Md Shafiqul Islam[1,d], and Johan Pilthammar[1,2,e]

[1]Department of Mechanical Engineering, Blekinge Institute of Technology, Karlskrona, Sweden

[2]Volvo Cars Dept. 81110 Strategy & Concept, Olofström, Sweden

[3]AutoForm Development GmbH, Zurich, Switzerland

[a]Alexander.Barlo@bth.se, [b] mats.sigvant@volvocars.com, [c]niko.manopulo@autoform.ch, [d]mdm@bth.se, [e]johan.pilthammar@volvocars.com

Keywords: Formability, Failure Prediction, Path Dependency, Non-Linear Strain Paths

Abstract. An area in the automotive industry that receives a lot of attention today is the introduction of lighter and more advanced material grades in order to reduce carbon emissions, both during production and through reduced fuel consumption. As the complexity of the introduced materials and component geometries increases, so does the need for more complex failure prediction approaches. A proposed path-independent failure criterion, based on a transformation of the limit curve into an alternative evaluation space, is investigated. Initially, the yield criterion used for this transformation of the limit curve was investigated. Here it was determined that the criterion for the transformation could not be decoupled from the material model used for the simulation. Subsequently, the approach using the transformed limit curve was tested on an industrial case from Volvo Cars, but a successful failure prediction was not obtained.

Introduction

An area of automotive engineering that receives a large amount of attention today is how to reduce the carbon footprint of a vehicle throughout its entire lifetime. Within the departments that concerns the manufacturing of automotive body components, one approach to meet these demands is to introduce lighter and more advanced material grades into the production lines. It can be noted that lighter and stronger materials are often less formable. So, using these advanced materials plus the demand for more complex shaped parts push recent designs to reach very close to the forming limit of the materials in some regions of the part. This naturally makes accurate failure prediction crucial. The study presented in this paper will investigate a path independent failure criterion, originally proposed by Zeng et al. [1] on a component from Volvo Cars that has proven to fail due to non-linear strain paths (NLSP). This paper will start out with a walk-through of the investigated approach.

Method

The path independent failure criterion investigated in this paper was originally proposed by Zeng et al. [1] as an alternative to the stress-based forming limit diagram proposed by Stoughton [2]. The investigated approach relies on a transformation of the evaluation space for failure from the traditional principal strain space, defined by coordinates in minor and major strain, to a space defined by the material flow direction α at the end of forming and the effective plastic strain $\bar{\varepsilon}^p$. The foundation for the approach is, that the parameter α, defined as the relationship between the increment in minor and major strain for the last stage in simulation (see Eq. 1), is uniquely related to the stress ratio σ_2/σ_1 for an associated flow rule.

$$\alpha = \dot{\varepsilon}_2/\dot{\varepsilon}_1 \tag{1}$$

Industrial Case

For the investigation of the approach, an industrial case manufactured from a VDA239 CR4 mild steel is used. A component from Volvo Cars has been chosen (see Fig. 1), as the component has proven to fail partially due to NLSP without this being detected in the simulations using the standard failure prediction approaches in an industrial setting.

Fig. 1: Volvo Cars component showing failure due to Non-Linear Strain Path.

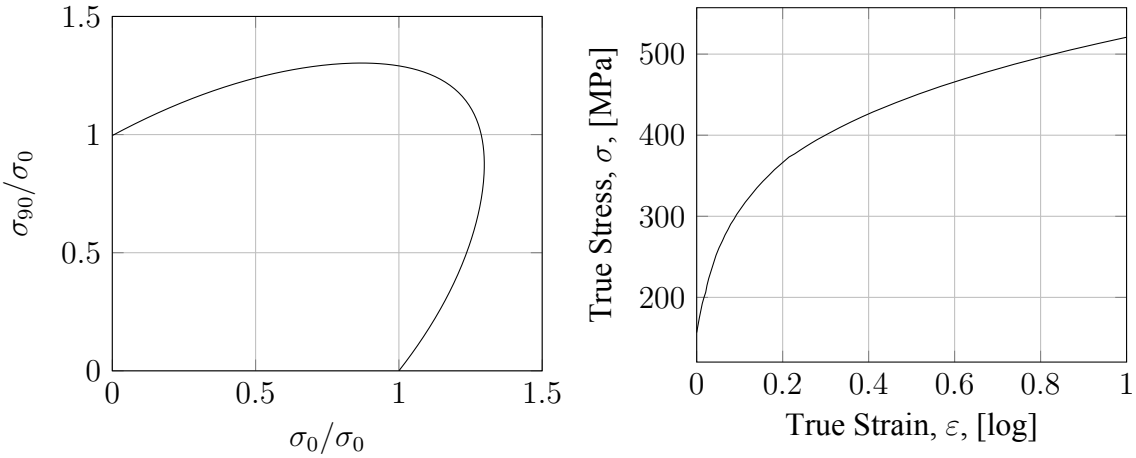

Fig. 2: Yield locus and hardening curve of the VDA239 CR4 mild steel.

Table 1: Parameters for the BBC 2005 Material Model

r_{00}	r_{45}	r_{90}	r_b	σ_0/σ_0	σ_{45}/σ_0	σ_{90}/σ_0	σ_b/σ_0	M
1.805	1.336	1.876	0.982	1	1.0214	0.9959	1.1938	4.5

The component has been modelled in the Finite Element (FE) software AutoForm™ R10 with a BBC 2005 material model. Figure 2 presents the yield locus and hardening curve, and Table 1 presents the parameters for the BBC 2005 material model. In the FE software, the component was checked with the standard failure prediction tools. In AutoForm™ R10 an advanced version of the standard Forming Limit Diagram (FLD), based on the method proposed by Volk and Suh [3], is available. This advanced FLD should be able to account for NLSP, however when evaluating the industrial case with this tool, the component is marked safe (see Fig. 3), even if the necking curve is entered as the limiting

criteria. The strain path presented in Figure 3 is that of the critical element where the crack appears. What should be noted is that the loading path changes with respect to the rolling direction. One of the requirements for the application of the advanced FLD is that such change does not occur. This results in a change from uniaxial load condition in the rolling direction to a plane strain load condition in the rolling direction is assumed to be the same as a change from uniaxial load condition in the rolling direction to a plane strain load condition in the transverse direction. In the industrial case presented in this paper, we can perform a check of the standard FLC and advanced FLC by looking at the Max Failure feature in AutoForm™ R10. The Max Failure feature measures how close one is to the limit curve of the standard FLC and the advanced FLC. The Max Failure value for the critical element for the standard FLC is 0.822, and for the advanced FLC it is 0.854. This indicates, that the advanced FLC do account for the non-linearity of the strain path, but it is ignoring the change with respect to rolling direction, and therefore does not mark the critical element as critical. This challenging aspect of predicting failure in components exposed to changes in load path with respect to the rolling direction further strengthens the argument for research into prediction of failure due to NLSP.

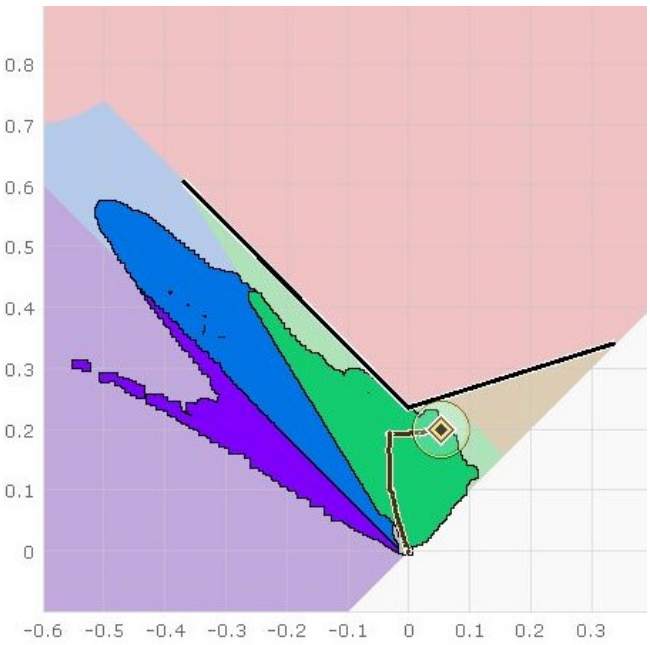

Fig. 3: Evaluation of the industrial case using the Advanced Forming Limit Diagram available in AutoForm^{TM} R10. The strain path of the critical element is highlighted

Limit Curve Transformation

An integral part of the method by Zeng et al. [1] is the transformation of the standardized Forming Limit Curve (FLC) into the new evaluation space. In their paper, the transformation is performed using a Hill'48 material model for the calculation of the limit strain $\bar{\varepsilon}^p$. It is well known that the choice of yield criterion highly influences the calculation of i.e., the equivalent plastic strain. Since the industrial case is modelled with a BBC 2005 yield criterion, a study of how large the impact of the selected yield criterion for the transformation is on the limit strain will be conducted. Three different yield criteria will be looked into: von Mises, Hill'48, and BBC 2005.

The FLC used in the industrial case has been experimentally determined in compliance with ISO 12004-2 [4] and was recorded with the 3D DIC system ARAMIS from GOM. In the industrial case, the term 'failure' will be defined as the onset of localized necking. Therefore, the FLC is in this case describing the onset of localization. To accurately determine the point in the test where the onset of localization occurs, the method proposed by Sigvant et al. [5] was used. The FLC for the VDA 239 CR4 mild steel can be seen in Figure 4.

In order to perform the transformation, an assumption of linear (and proportional) deformation from zero to limit strain is made so that $d\varepsilon_i = \varepsilon_i$. Table 2 presents the experimental points of the FLC.

Table 2: Experimental Forming Limit Curve points.

FLC Point [-]	**Major Strain, ε_1, [log]**	**Minor Strain, ε_2, [log]**
Uniaxial Tension	0.608	-0.370
Plane Strain	0.235	0.000
Equi-biaxial Tension	0.341	0.340

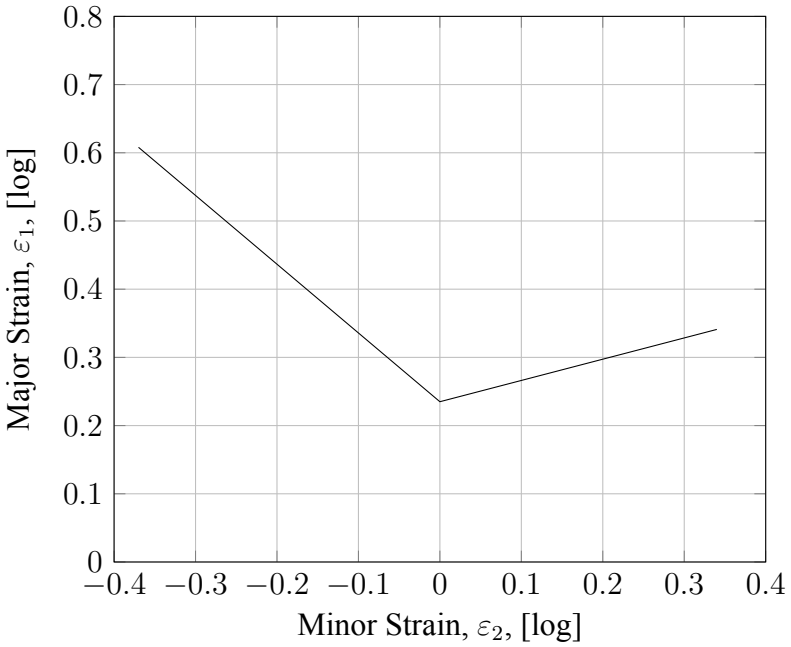

Fig. 4: Necking limit of the VDA239 CR4 mild steel. The curve is determined experimentally in compliance with ISO 12004-02 [4] and the onset of localized necking is determined according to the method proposed by Sigvant et al. [5].

For the transformation, the number of data points in the FLC has been expanded from 3 to 49 by evenly distributing 25 points between the uniaxial and plane strain points, and another 24 between the plane strain and equi-biaxial point. This is done due to observations made in the transformed curves of Zeng et al. [1] and Mattiasson et al. [6] where the limit curve cannot be defined by two linear sections between the uniaxial and plane strain point and the plane strain point and the equi-biaxial point. For the first transformation, the von Mises yield criterion is used. For the calculation of the von Mises equivalent plastic strain, an assumption of associated flow rule and plane stress is made, leading to the expression presented in Eq. 2 can be used.

$$\overline{\varepsilon}^p = \sqrt{\frac{4}{3} \cdot (\varepsilon_1^2 + \varepsilon_2^2 + \varepsilon_1 \cdot \varepsilon_2)} \tag{2}$$

For the transformation using the Hill'48 yield criterion, Eq. 3 is used to calculate the equivalent plastic strain [7]. For this calculation an assumption of linear deformation ($d\varepsilon_i = \varepsilon_i$) and plane strain ($\varepsilon_{12} = 0$) is made.

$$\overline{\varepsilon}^p = \sqrt{\frac{1}{F \cdot H + F \cdot G + G \cdot H} \cdot [(F + H) \cdot \varepsilon_1^2 + 2 \cdot H \cdot \varepsilon_1 \cdot \varepsilon_2 + (G + H) \cdot \varepsilon_2^2]} \tag{3}$$

For the Hill'48 determination, the three constants F, G, and H can be determined based on the r-values according Eq. 4 [8].

$$
\begin{aligned}
R_{22} &= \sqrt{\frac{r_{90}\cdot(r_{00}+1)}{r_{00}\cdot(r_{90}+1)}} \\
R_{33} &= \sqrt{\frac{r_{90}\cdot(r_{00}+1)}{r_{00}+r_{90}}} \\
F &= \frac{1}{2}\cdot\left(\frac{1}{R_{22}^2}+\frac{1}{R_{33}^2}-1\right) \\
G &= \frac{1}{2}\cdot\left(-\frac{1}{R_{22}^2}+\frac{1}{R_{33}^2}+1\right) \\
G &= \frac{1}{2}\cdot\left(\frac{1}{R_{22}^2}-\frac{1}{R_{33}^2}+1\right)
\end{aligned}
\tag{4}
$$

For the transformation of the curve using the BBC 2005 yield criteria this is not possible to do analytically why a numerical approach must be adapted. For this, the approach presented by Bandpay [9] is used to calculate the equivalent plastic strain of the different points of the standard FLC.

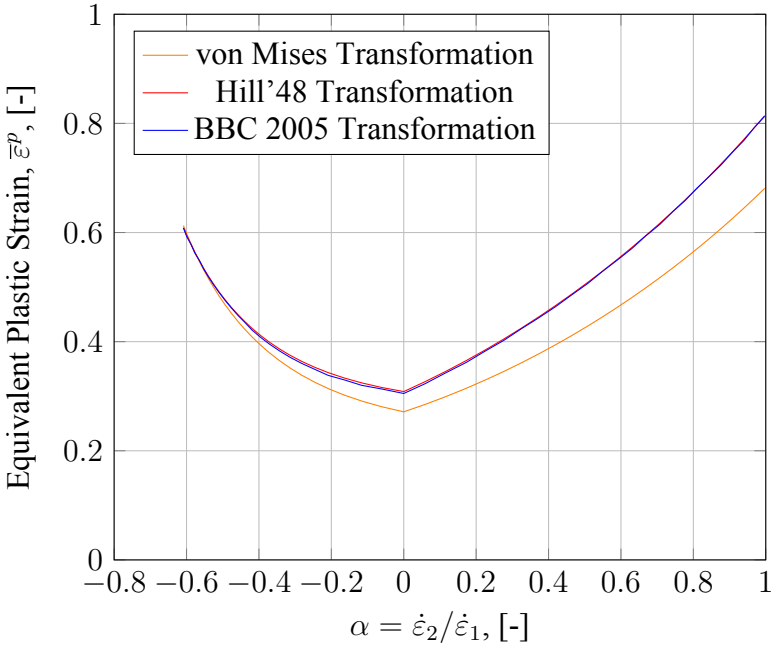

Fig. 5: Forming Limit Curve transformed from the traditional principal strain space into the new evaluation space based on three different yield criteria.

Figure 5 presents the transformed curves based on the three different yield criteria. As expected, the limit curve generated based on the von Mises yield criterion performs way different that those of the Hill'48 and BBC 2005 criteria. Focusing on the other two limit curves, they are highly similar, with the limit curve transformed based on BBC 2005 slightly lower, most prominent in the area of plane strain ($\alpha \approx 0$). This behavior seems to be in line with how the yield locus behaves with the two different criteria. Figure 6 presents a comparison of the yield loci when applying the Hill'48 and BBC 2005 criteria. From this, it can be seen that the two loci correspond very well to each other except in the region describing the plane strain behavior of the material. Therefore, to make an educated decision on which model to choose in this case, experimental data from a Limiting Dome Height (LDH) test is compared to simulations using a Hill'48 and BBC 2005 yield criteria.

Figure 7 presents a comparison of the major and minor strain profiles over a cross section of the experimental data (experiments of same batch of material as for the industrial case) and simulations run with Hill'48 and BBC 2005 yield criteria presented by Sigvant and Pilthammar [10]. This clearly shows that the BBC 2005 yield criteria predicts the strains better than the Hill'48. Due to this, the limit curve determined using the BBC 2005 yield criteria will be used for the post-processing.

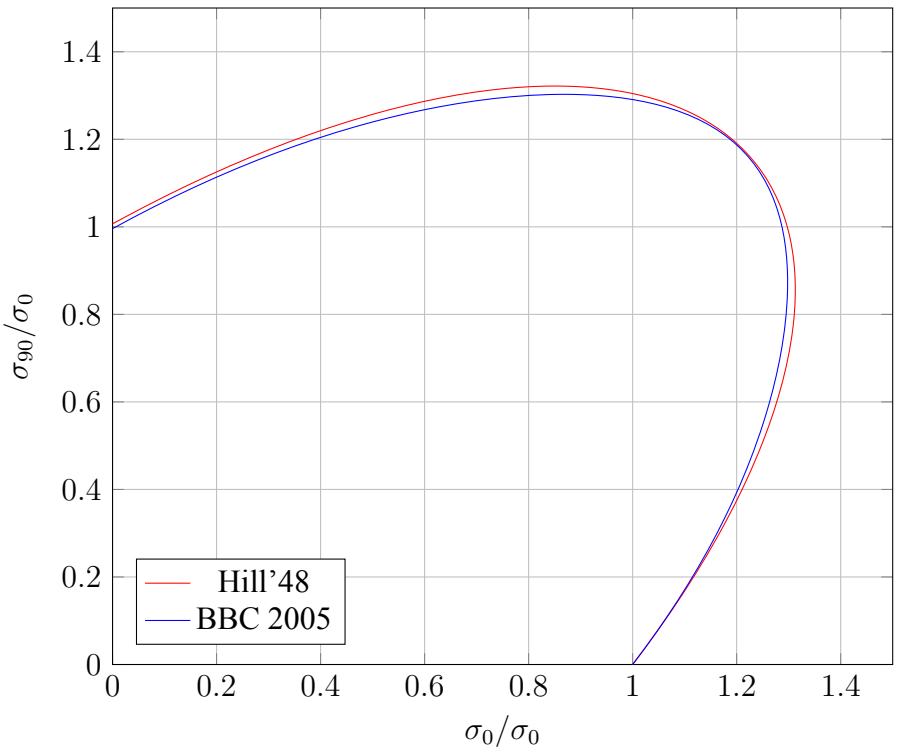

Fig. 6: Comparison of the yield loci for the VDA239 CR4 mild steel when applying a Hill'48 and BBC 2005 material model.

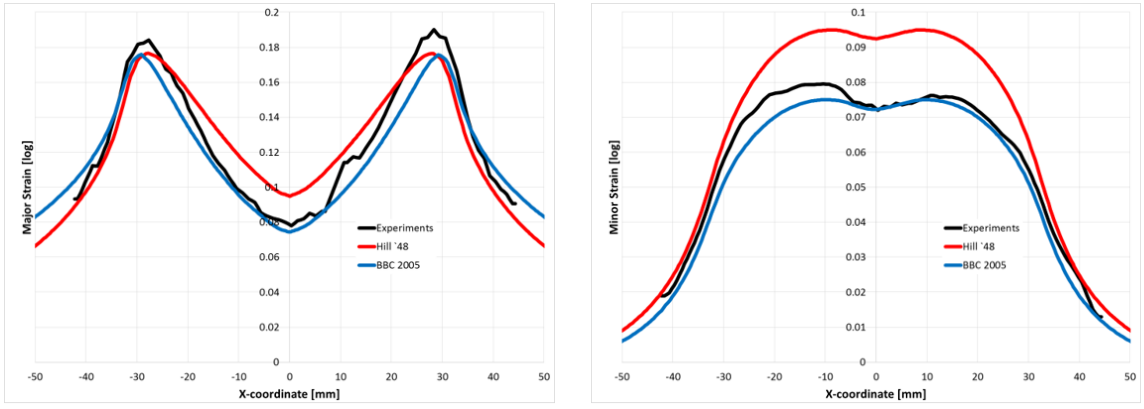

Fig. 7: Strain profile over a cross-section of a LDH-test of the VDA239 CR4 mild steel. Experimental results compared to simulations using Hill'48 and BBC 2005 yield criteria [10]

.

Post-Processing

The chosen curve based on the BBC 2005 yield criteria is applied to the industrial case from Volvo Cars. In order to do so, the strain paths of 5 different elements in the simulation are chosen to test the approach – one strain path from a critical element in the split area, and four arbitrary elements chosen in areas with high plastic strain values. The four arbitrary elements can be seen in Figure 8. These five different elements yield different strain paths – some highly non-linear and some resembling more linear strain paths (Figure 9). This mix of strain paths is deemed to be a good fit for a first test of the method, as it is important that the method does not create 'false positives' of failure where other approaches mark the point safe (*concept of primum non nocere – first do no harm* [11]). Especially interesting is the strain path for the critical element.

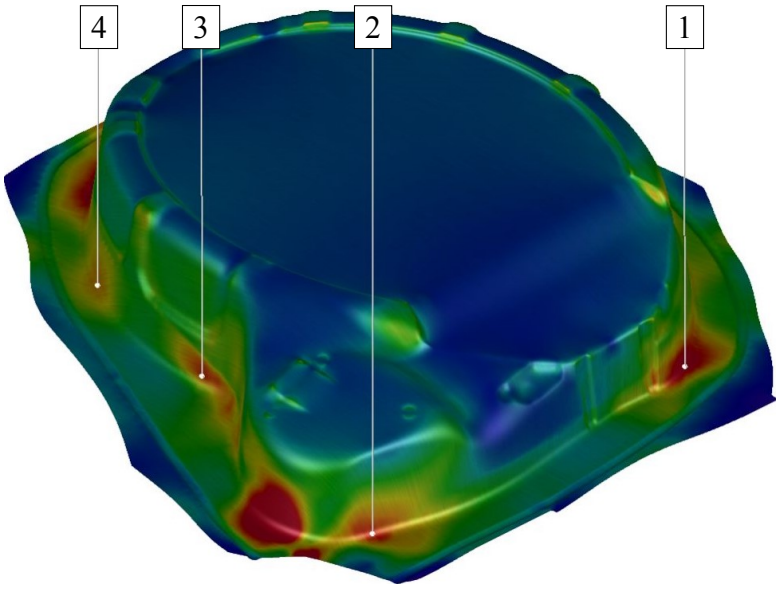

Fig. 8: Arbitrary control elements in areas with high plastic strain values.

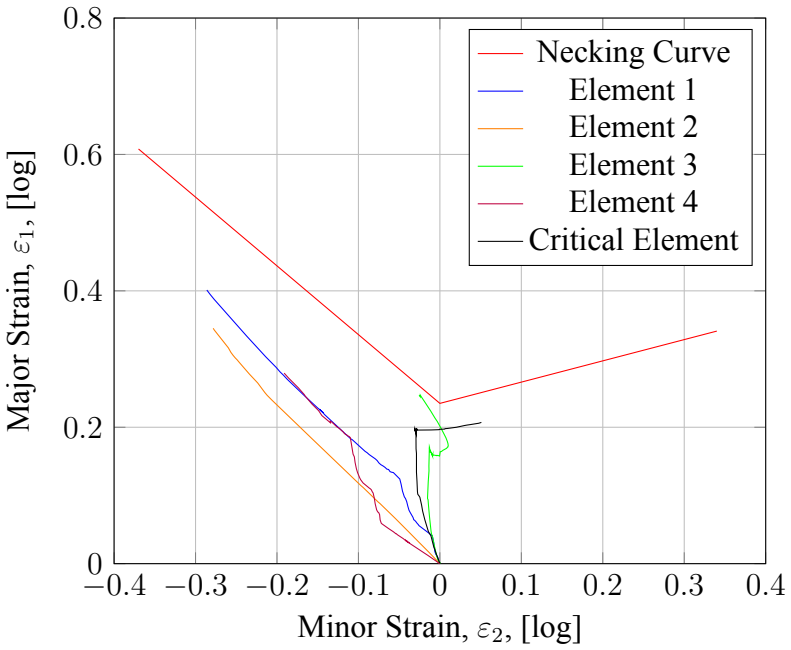

Fig. 9: Strain paths of the critical element and the four arbitrary control points in the principal strain space.

The critical points start out by being formed under plane strain condition up to roughly 20%. From here the strain path does a near 90° turn and proceeds to have a very small increase in major strain value in the principal strain space. The critical element ends up being relatively far away from the necking curve, especially compared to element 3. However, in reality element 3 does not fail, and the critical element not only show sign of onset of necking, it produces a through-thickness crack as presented in Figure 1.

As with the limit curve, the 5 elements investigated also needs to be transformed from the principal strain space. The equivalent plastic strain in the element is simply obtained from the simulation and exported so a post-processing can occur outside the FE software. The calculation of the α value is based on major and minor strains also exported from the FE software. According to Zeng et al. [1] and Mattiasson et al. [6], the path independence of the approach comes from the strong link to the stress-based forming limit diagram. This is backed up by Stoughton and Zhu [12] arguing that this is due to the path-independent constitutive laws governing the evolution of stresses and strains. Therefore, for the evaluation, the full strain path need not to be considered, but only the last step of the simulation. The data for the arbitrary and critical elements both in the principal strain space and the transformed evaluation space can be found in Table 3, and a plot of evaluation space can be seen on Figure 10.

Table 3: Data for the arbitrary and critical elements in the principal strain space and the transformed evaluation space.

Parameter	Element 1	Element 2	Element 3	Element 4	Critical Element
ε_1(i) [log]	0.4012	0.3451	0.2473	0.2794	0.2071
ε_1(i-1) [log]	0.4003	0.3446	0.2465	0.2791	0.2069
ε_2(i) [log]	-0.2861	-0.2783	-0.0255	-0.1912	0.0509
ε_2(i-1) [log]	-0.2856	-0.2780	-0.0251	-0.1911	0.0503
α [-]	-0.5453	-0.5712	-0.4407	-0.3754	2.6576
$\bar{\varepsilon}^p$ [log]	0.4320	0.3608	0.3621	0.3125	0.3477

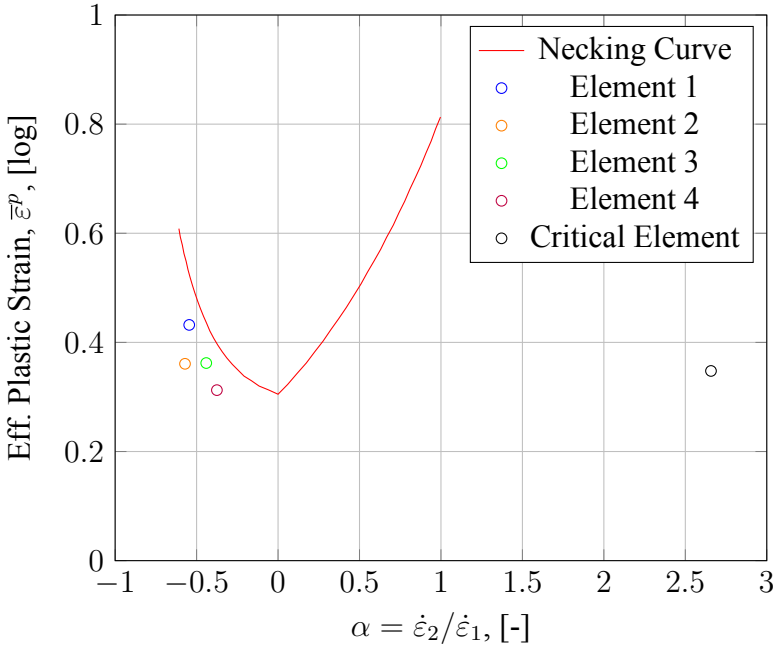

Fig. 10: Illustration of the arbitrary and critical elements in the transformed evaluation space

From Figure 10 it is clear that the approach highly overpredicts the α-value of the critical element. The α-value in the plot should not be able to pass the value of 1 since this indicates an equi-biaxial

strain state. What is seen here could be the result of the near 90° turn in the critical strain path, which could be an extremely rare phenomenon that needs to be discussed further. The positive outcome of the investigation is that for the four arbitrary control elements selected, no false positives are detected.

Discussion

As presented, the investigated approach was not able to predict the failure in the critical strain path of the industrial case. This does not necessarily mean that the approach should be discarded immediately. Taking a closer look at the strain path of the critical point (Fig. 9), the near 90° turn in the path is what is expected to cause trouble. The critical strain path starts out in a plane strain condition up until the turn. After the turn, the path could be interpreted so that a plane strain condition is present, but in a different direction than of the first part. According to Mattiasson et al. [6] the only parameters that matter is the plastic strain and the plastic flow direction. With the assumption of associated flow rule, the plastic flow direction is equivalent to the normal to the yield locus. Figure 11 outlines the value of α at different locations on the yield locus.

As presented in Figure 11, at the equi-biaxial point, α will take the value of 1. From here, the α value will increase until the horizontal tangent of the yield locus where α is infinitive. Continuing towards uniaxial stress, a negative normal is present and therefore α will be less than zero. The green arrow on Figure 11 indicates the jump the critical strain path takes when performing the turn. The script used for the post-processing in this study does not account for the fact that the point passes over the theoretical maximum value of α. Some sort of correction for this behavior should be implemented. One approach could be to assume the yield locus to be double symmetric and bounding the α-value between -1 and 1. How this should be handled when α practically passes 1 needs to be investigated further.

Furthermore, when assessing the formability of a component with a strain path as the one presented in this study, the influence of the material anisotropy should not be neglected. The limit curve presented in Figure 4 has been determined with test specimens cut along the transverse direction. With a change in the loading direction the limit used to assess the remaining formability should also be altered as presented by Volk et al. [13].

Lastly, another concern that needs to be addressed is the fact the approach relies on the strain increments for the calculation of α. This could potentially mean that the approach is highly sensitive to the step size in the model. However, no investigation of this has been carried out in this study, why it is a topic for further discussion.

Conclusion

A path-independent approach to predict failure due to non-linear strain paths proposed by Zeng et al. [1] was investigated. As the proposed method relies on a transformation of the evaluation space from the principal strain space into an evaluation space defined by the equivalent plastic strain and the material flow direction, it was initially investigated if the yield criterion used for the transformation of the Forming Limit Curve could be decoupled from the material model used for the simulation. Three different yield criteria were tested for the transformation of the limit curve: von Mises, Hill'48, and BBC 2005. It was concluded that even though the curves generated with the Hill'48 and BBC 2005 yield criteria were highly similar, the study should move forward with the one generated by using the BBC 2005 criteria to match what was used in the simulation. This conclusion was reached after consulting a comparison of the yield loci of the two criteria for the material, as well as major and minor strain predictions compared to experimental data of a Limiting Dome Height (LDH) test. Therefore, it was concluded that the yield criteria for the transformation of the limit curve could not be decoupled from the material model used for the simulation.

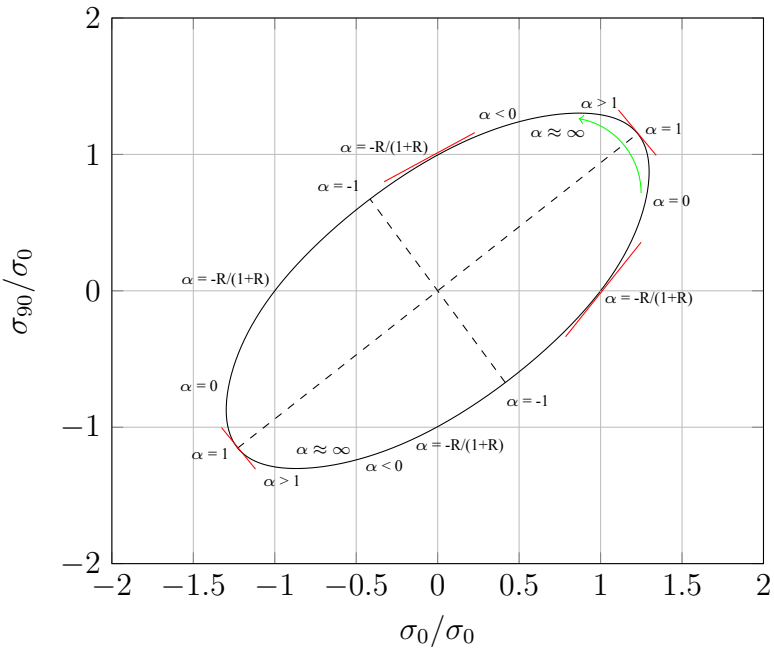

Fig. 11: Illustration of different α-values on different locations of the yield surface. When the 90° occurs in the critical strain path, the element jumps on the yield locus following the green arrow.

Furthermore, the approach using the transformed path-independent limit curve was tested on an industrial case from Volvo Cars that had produced a through thickness crack partially due to nonlinear strain paths. Four arbitrary elements, chosen to check for false positives, and the critical element of the simulation were all tested against the transformed limit curve. None of the elements indicated failure, why initially the approach has failed. However, due to the strange nature of the strain path of the critical element, it was argued that the approach should not be discarded before further investigation into the phenomena of radical turns in the strain path has been investigated.

Acknowledgements

Open Access funding was provided by Blekinge Institute of Technology. This study was also funded by VINNOVA in the Sustainable Production sub-program within Vehicle Strategic Research and Innovation (FFI) program (grant number 2020-02986).

References

[1] D. Zeng, L. Chappuis, Z. C. Xia and X. Zhu, A Path Independent Forming Limit Criterion for Sheet Metal Forming Simulations, SAE Int. J. Mater. Manu, Vol. 1, No. 1 (2009), pp. 809-817.

[2] T. Stoughton, A general forming limit criterion for sheet metal forming, Int. J. Mech. Sci. 42 (2000), pp. 1-27.

[3] W. Volk and J. Suh, Prediction of formability for non-linear deformation history using generalized forming limit concept (GFLC), AIP Conference Proceedings 1567 (2013), pp. 556-561.

[4] International Standard Organization, Metallic Materials – Determination of Forming-Limit Curves for Sheet and Strip – Part 2: Determination of Forming-Limit Curve in the Laboratory (ISO 12004-2) (2008).

[5] M. Sigvant, K. Mattiasson and M. Larsson, The Definition of Incipient Necking and its Impact on Experimentally or Theoretically Determined Forming Limit Curves, 2008 IDDRG Conference Proceedings, 16-18 June, Olofström, Sweden (2008).

[6] K. Mattiasson, J. Jergéus, and P. DuBois, On the prediction of failure in metal sheets with special reference to strain path dependence, Int. J. Mech. Sci. 88 (2014), pp. 175-191.

[7] R. B. Colby, Equivalent Plastic Strain for the Hill's Yield Criterion under General Three- Dimensional Loading, Bachelor Thesis, Massachusetts Institute of Technology (2013).

[8] D. Banabic, Sheet Metal Forming Processes: Constitutive Modelling and Numerical Simulation, Springer Berlin Heidelberg (2010).

[9] M. G. Bandpay, Instability and Fracture Models to Optimize the Metal Forming and Bending Crack Behavior of Al-Alloy Composites, PhD Thesis, ETH Zurich (2015).

[10] M. Sigvant and J. Pilthammar, Sheet Metal Forming Simulations at Volvo Cars: The past, the present and the future, Keynote presentation, Forming Technology Forum (2019), Munich, Germany.

[11] N. Manopulo and B. Carleer, On the way towards a comprehensive failure modelling for industrial sheet metal stamping processes, IOP Conf. Ser.: Mater. Sci. Eng. 651 (2019), pp. 012004.

[12] T. Stoughton and X. Zhu, Review of theoretical models of the strain-based FLD and their relevance to the stress-based FLD, Int. J. Plast. 20 (2004), pp 1463-1486.

[13] W. Volk, M. Gruber and R. Norz, Prediction of limit strains during non-proportional load paths with a change in loading direction, IOP Conf. Series: Mater. Sci. Eng. 967 (2020), pp. 012069.